Dynamic temperature supply to boost the integration of renewable energy into existing district heating networks

Renewable Energy 256 (2026) 124315

Contents lists available at ScienceDirect

Renewable Energy

journal homepage: www.elsevier.com/locate/renene

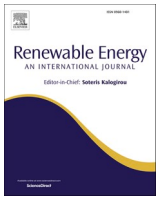

Dynamic temperature supply to boost the integration of renewable energy into existing district heating networks

Martina Capone *, Marco Canino, Elisa Guelpa

Politecnico di Torino, Energy Department, Turin, Italy

ARTICLE INFO

Keywords:
Renewable heat
Low temperature heating
Network model
Thermal substation
Groundwater heat pump
Thermal grid

ABSTRACT

The integration of renewable energy into District Heating systems is essential to achieving decarbonization targets by 2050. The transition to low-temperature renewable sources may be challenging in the case of large-scale systems originally designed for high-temperature fossil fuel plants. In this study, the implementation of a dynamic temperature supply strategy in portions of the network is proposed as a convenient solution to promote the integration of renewable energy and the transition to low temperature operation in existing networks. This objective is pursued through the installation of decentralized production units that use groundwater heat pumps and deliver hot water at lower temperature level than those of the central plant, which continues to operate just as a booster unit. The feasibility of the proposed operating conditions is evaluated by means of a physical model, which includes both the simulation of the network operation and a representation of the behavior of the different buildings. The application is tested on three sub-networks within a real large-scale system in Northern Italy. The results show that for more than 50 % of the operating time, the sub-networks can be supplied at temperatures between 40 °C and 90 °C using renewable energy, with the central fossil-fuel-based plant providing support only during the most demanding conditions.

1. Introduction

Decarbonizing the energy sector requires rapid progress to meet the European targets and to achieve climate neutrality by 2050 [1]. Efforts must extend to all sectors, including the heating and cooling sector: although it has received less attention than power generation [2], this sector plays a key role in the transition, as it accounts for the largest share of global energy consumption [3].

District Heating (DH) is recognized as a key technology for the transition to a low-carbon energy system [4,5], as it facilitates heat recycling and the use of renewable heat, thus reducing the environmental impact compared to conventional heating methods [6]. A significant advantage of DH is its ability to integrate the thermal network with the electricity grid and other energy infrastructures through appropriate conversion plants [7]. By exploiting the synergies between these interconnected infrastructures, the overall energy system can be optimized, enabling efficient management and contributing to the common goal of reducing emissions [8].

In this context, integrating heat pumps (HPs) into DH systems offers a promising solution, adding flexibility to both the power grid and the heating network [9,10]. HPs can be installed both as small-scale and large-scale solutions [11]: the latter offers numerous advantages, including the potential of exploiting strategic heat sources [12]. While outdoor air-sourced HPs are the easiest types of systems to install, the use of site-specific heat sources such as water or ground is more convenient due to higher efficiencies and can be efficiently implemented in DH networks [13]. The deployment of these technologies is expected to further grow in the future, as the development of DH towards lower temperature further improves the coefficient of performance (COP) of HPs [14].

The reduction of operating temperatures represents one of the biggest challenges in upgrading existing DH networks. In fact, many DH networks in operation today were designed to operate at high temperatures, which were readily available from traditional fossil fuels. However, the move to renewable generation and the transition to fourth-generation DH now requires a decrease in temperature levels [15]. Although the current temperature levels in existing systems are often too high with respect to the final heat demands [16], transitioning to lower

This article is part of a special issue entitled: SI ECOS2024 published in Renewable Energy.

* Corresponding author.
E-mail address: martina.capone@polito.it (M. Capone).

https://doi.org/10.1016/j.renene.2025.124315
Received 7 February 2025; Received in revised form 2 May 2025; Accepted 27 August 2025
Available online 29 August 2025

temperatures may be a long and complex process, especially in the case of large-scale infrastructures. Huge temperature reductions may not be supported by systems designed to operate under different conditions, due to many limitations that can occur at the building, substation, or network level [17]. Nevertheless, these systems cannot be replaced to target cost-effective decarbonization of the energy system. Therefore, strategies to boost temperature reductions in this existing infrastructure need to be pursued [18–20].

To overcome the techno-economical issues associated with a full transformation of the existing infrastructure, the implementation of low temperature sub-networks (sub-LTDH) was proposed as a possible solution to gradually improve the efficiency of the systems [21–24]. These systems consist of small sub-networks, operating at low temperatures, connected to a master DH network with higher temperatures. Either the return temperature of the master DH network can be used to meet the thermal demands of the connected buildings, or they can have additional dedicated heat sources, while the use of the supply flow of the master network is limited to cover peak demands [22].

This work discusses the implementation of sub-LTDH as a practical solution for facilitating the integration of distributed renewable energy sources into existing DH networks. The complete system is depicted in Fig. 1: the master network, operating at high temperatures, is supplied by centralized plants; in sections of the network currently operating at high temperatures, distributed generation units installed at the sub-network level can lower the supply temperature and enable renewable integration. The sub-LTDHs remain connected to the master network, which continues to provide support when needed by supplying a variable fraction of high-temperature mass flow to mix with the low-temperature supply from the renewable generation unit.

In this paper, groundwater heat pumps (GWHPs) are considered as generation units for the sub-LTDH as an opportunity to exploit the potential of geothermal resources in suitable areas [25,26]. Nevertheless, the methodology presented in this work is replicable also considering different production sources. GWHPs are geothermal open-loop systems that have become particularly attractive in DH applications due to their relatively low cost [27] and efficiency [28]. A schematic representation of the system configuration is given in Fig. 2: the HP uses groundwater extracted through a production well as heat source: in the heating mode, the groundwater releases heat to the working fluid of the HP through the evaporator, and it is reinjected with a slightly lower temperature in the ground. The temperature level of this heat is increased by the heat pump, and through the condenser of the HP, the mass flow rate in the DH network can be heated up to the supply temperature.

Within this framework, this work aims to develop a methodology to assess the feasibility of implementing the described sub-LTDH configuration, taking into account:

- The evolution of the heat demand of the different buildings connected to the sub-networks over the years.
- The operation of the thermal substations, simulated by a dedicated model. The model makes it possible to simulate the operation of each substation with reduced flow temperatures, in order to estimate the increase in mass flow required to compensate for the temperature reduction in order to meet the required thermal demand and comply with the temperature requirements.
- The thermo-fluid dynamic response of each sub-LTDH. A physical model of the distribution network is adopted to predict the evolution and distribution of mass flow rates, pressures, and temperatures in the entire network. This is essential to guarantee the sustainability of the increased mass flow rates and velocities in the network, to accurately predict the supply temperatures of the substations, and to be able to estimate the operating conditions of the distributed generation unit.

Through this methodology, the minimum supply temperature of a given sub-LTDH under different operating conditions can be determined. Finally, a simplified model of the GWHP allows a) to estimate the performance of the unit, b) to analyze the interface with the master network, and c) to assess the potential of renewable energy integration into an existing DH network.

The methodology is applied to an existing large-scale network located in Northern Italy and currently operating with high supply temperatures. Three subsystems are selected for the analysis, which is carried out over 8 years of operation.

After this introductory section, the remaining part of the paper is structured as follows:

- Section 2 is dedicated to the explanation of the methodology;
- Section 3 introduces the case study;
- In Section 4, the results of the analysis are presented and discussed;
- Finally, Section 5 summarizes the main conclusions of the work.

2. Methodology

This work proposes a methodology to assess the feasibility of the implementation of sub-LTDH with GWHPs into existing DH systems. This consists of two parts:

1. The first part of the methodology (Section 2.1) focuses on simulating the operation of the subsystem at reduced temperature. A dynamic temperature approach is proposed, which involves varying the supply temperature of the sub-LTDH according to the thermal demand and to the temperature level required in each condition.
2. The second part (Section 2.2) addresses the evaluation of the performance of the GWHP.

2.1. Simulation of the sub-LTDH at reduced temperature

In this section, the dynamic temperature approach is discussed and the methodology adopted to simulate the new operating conditions is described.

The proposed strategy involves dynamically adjusting the supply temperature of the network based on the demand under specific

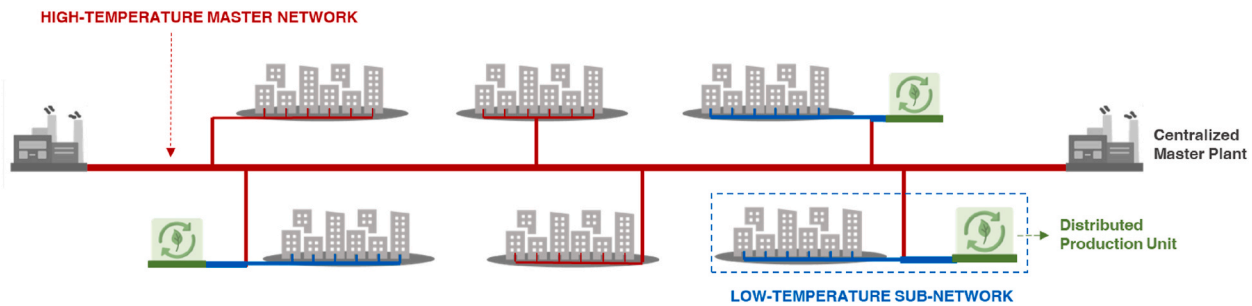

Fig. 1. Representation of the system: high-temperature master network and low-temperature sub-networks (sub-LTDH).

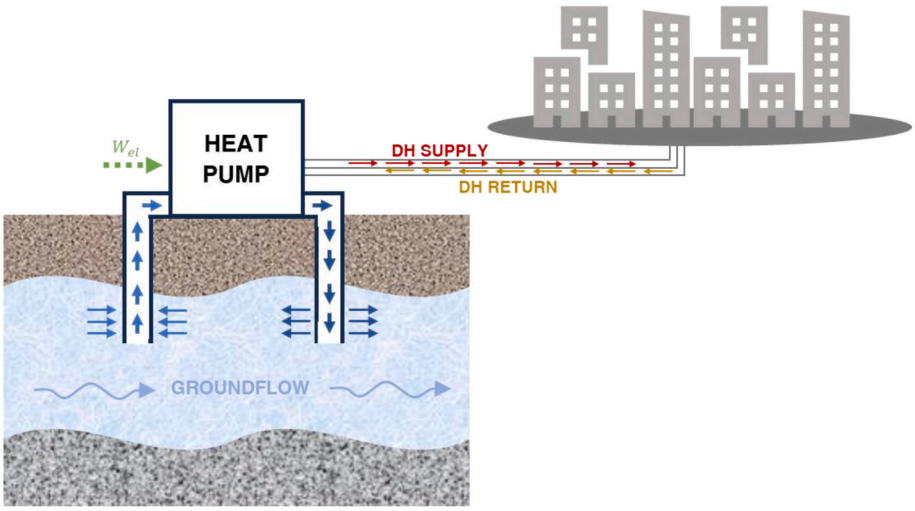

Fig. 2. Schematic representation of a GWHP connected to a DH network.

operating conditions. While typically the supply temperature of the network remains constant, with the mass flow rate controlled to match the demand of the customers, in this approach the supply temperature is reduced to the lowest value allowed by the network in each condition.

A steady-state simulation model is developed to determine the lowest temperature allowed in each system. The model is used to simulate the operating conditions over a relevant period of time and includes:

- a black box model of the buildings to estimate their thermal demand based on the outdoor temperature (Section 2.1.1);
- a grey box model of the thermal substations to obtain the mass flow rate that is needed to satisfy the required thermal demand with a given supply temperature on the network side (Section 2.1.2);
- a physical model of the DH network to calculate the temperature drops in the network according to the mass flow rates required by the different buildings and to perform a thermo-fluid dynamic analysis of the system (Section 2.1.3).

The model is repeated within an iterative process: starting from a very low network supply temperature, this value is increased if it is not sufficient to satisfy the demand of the entire sub-LTDH. Another iterative process is required because of the interdependence of the substation and network models: indeed, the mass flow rate required by each building depends on the supply temperature of the substation on the network side according to the substation model, but at the same time the supply temperature of the substation on the network side is an output of the network model, which requires as input the mass flow rate of all the substations. More details about the structure of the model will be given in Section 2.1.4.

The proposed model requires the availability of a sufficient amount of data:

- Temperature data from the DH network and the building-side of thermal substations, as well as the primary-side mass flow rate, are necessary for calibrating the black-box and grey-box models. This data is typically collected by the DH operator for billing purposes.
- Knowledge of the network topology is required to perform the thermo-fluid dynamic analysis.

2.1.1. *Estimation of the thermal demand of the buildings*

The first step of the analysis involves estimating the thermal demand of each building connected to the network. This is achieved using a black-box model, which relates the heat demand Φ of each i-th building at a specific time t to the outdoor temperature in that time T^t_{out} through a linear function, as shown in Equation (1).

$$\Phi^t_i = f_i\left(T^t_{out}\right) = a_i T^t_{out} + b_i \tag{1}$$

The coefficients a_i and b_i are determined using linear regression applied to the data available at substation level. This process is illustrated in Fig. 3, where steady-state conditions are identified and isolated using an algorithm that monitors variations in the heat demand.

The linear regression models obtained are then used to estimate the thermal demand of each building, giving as input the outdoor temperature in the period of interest for the simulation. The values obtained from the model are subsequently constrained by a minimum and a maximum threshold, which can be easily noticed in Fig. 3 and corresponds to the minimum and maximum value of mass flow rate allowed by the substation valves; consequently, the allowable heat transfer range depends on the supply temperature of the substation, according to the model explained in Section 2.1.2.

The entire analysis is performed under steady-state conditions; it is assumed that the transient conditions – evident during the start-up phase of the systems following the night setback – can be managed using peak shaving techniques. For this reason, the daily operating hours are extended to ensure that the thermal energy supplied matches the building's energy demand throughout the day, as evaluated using a comparable linear regression model.

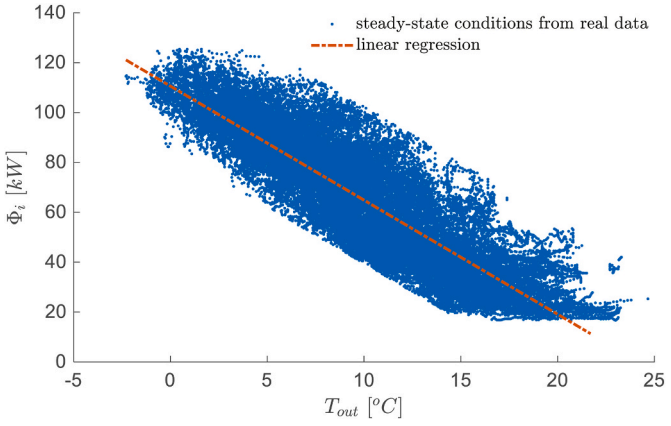

Fig. 3. Evaluation of the linear regression model used to estimate the steady-state heat load as a function of the outdoor temperature.

2.1.2. Model of the thermal substation

In this section, the model developed to simulate the operation of the substation at reduced supply temperature is described. It is a grey box model, combining a theoretical structure with data analysis to estimate the unknown characteristics of the substations. A conservative assumption of this analysis is that the substations continue to be simulated in the same state as they are currently operating, without considering the possibility of retrofitting interventions that would further improve the operation of the system.

The core structure of the substation model has been previously presented in Ref. [29]. Unlike the previous work, this paper extends the model to simulate not only the design conditions but also the off-design operating conditions over a full year. Additionally, the model is combined with the network model to provide a comprehensive representation of the system operation.

The thermodynamic equations included in the model are summarized in Equation (2). These equations incorporate energy balances across both sides of the substation, along with relationships derived from the effectiveness-NTU method [21]. As illustrated in Fig. 4, for each i-th building at the time step t:

- $\dot{m}_{p,i}^{t}$ represents the mass flow rate on the DH network side (primary side);
- $\dot{m}_{s,i}$ represents the mass flow rate on the building side (secondary side), whose value is derived from data analysis;
- c_p is the specific heat capacity of water, assumed as constant;
- $T_{1.i}^{t}$ and $T_{2.i}^{t}$ are the supply and return temperatures of the substation on the primary side, respectively;
- $T_{3.i}^{t}$ and $T_{4.i}^{t}$ are the supply and return temperatures on the secondary side, respectively;
- $T_{ind,i}^{t}$ is set-point temperature of the indoor environment.

Additionally, $\varepsilon_{I,i}^{t}$ and $\varepsilon_{II,i}$ represent the effectiveness of the substation heat exchanger and of a fictitious heat exchanger (used to model the collective performance of all heating devices within the building), respectively. Both effectiveness values are derived from data regression for each substation, enabling accurate estimation even when the heat exchanger area is not known a priori. While $\varepsilon_{II,i}$ is assumed constant over the entire simulation period, $\varepsilon_{I,i}^{t}$ is treated as a function of the primary-side mass flow rate $\dot{m}_{p,i}^{t}$ introducing additional nonlinearity into the system of equations. This is due to the dependence of $\varepsilon_{I,i}^{t}$ on the global heat transfer coefficient $U_{I,i}^{t}$, which is strongly dependent on primary-side mass flow rate. Readers interested in the data regression model used to estimate of $\dot{m}_{s,i}$, $\varepsilon_{I,i}^{t}$ and $\varepsilon_{II,i}$ are referred to Ref. [29].

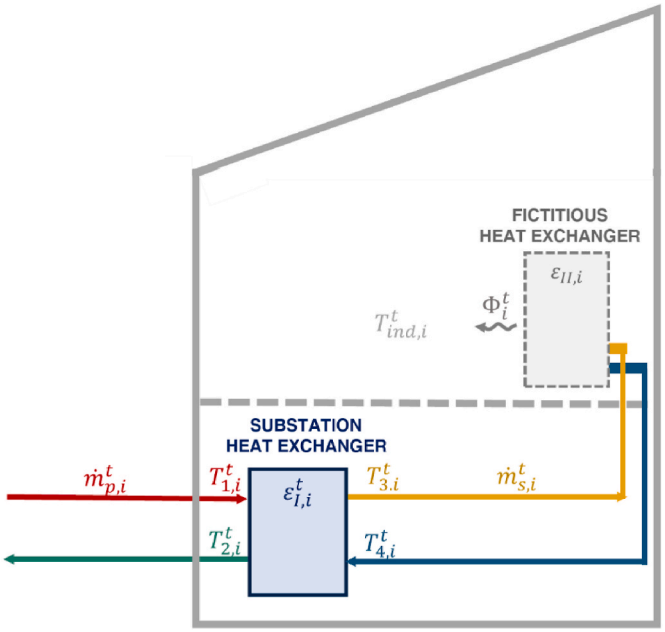

Fig. 4. Schematic representation of the substation model.

$$\begin{cases} \Phi_i^t = \dot{m}_{p,i}^t c_p \left(T_{1,i}^t - T_{2,i}^t\right) \\ \Phi_i^t = \dot{m}_{s,i}^t\, c_p \left(T_{3,i}^t - T_{4,i}^t\right) \\ \Phi_i^t = \varepsilon_{I,i}^t\, \dot{m}_{p,i}^t\, c_p \left(T_{1,i}^t - T_{4,i}^t\right) \\ \Phi_i^t = \varepsilon_{II,i}\ \dot{m}_{s,i}^t\, c_p \left(T_{3,i}^t - T_{ind,i}^t\right) \end{cases} \tag{2}$$

The substation model uniquely relates mass flow rates and supply temperature to the heat transfer, the return temperature, and the temperatures on the secondary side, based on the characteristics of the heat exchangers. Because of limitations on the mass flow rate, the heat transfer is limited to a maximum threshold, as reported in Equation (3), where $\dot{m}_{p,i}^{MAX}$ is the maximum primary-side mass flow rate allowed by the i-th substation.

$$\dot{m}_{p,i}^{t} \le \dot{m}_{p,i}^{MAX} \tag{3}$$

According to the substation model, as the supply temperature decreases, the temperature difference ΔT between the supply and return sides also decreases. Therefore, a higher mass flow rate is required to provide the same heat load; similarly, when the mass flow rate reaches its maximum limit, the heat transfer is reduced as the supply temperature decreases. As a consequence, certain operating conditions that are feasible in the current high-temperature scenario may not be feasible at reduced supply temperatures.

The complete set of equations and constraints described in this section and related to the grey-box substation model can be grouped into a compact form, as per Equation (4).

$$\left[\dot{m}_{p,i}^{t}, T_{2,i}^{t}, w_i^t\right] = g_i\left(T_{1,i}^{t}, \Phi_i^t\right) \tag{4}$$

The model takes as input the supply temperature of the substation on the network side $T_{1,i}^{t}$, which is an output of the supply network model, and the heat demand of the building in the analyzed time step Φ_i^t. As output, it provides the required mass flow rate $\dot{m}_{p,i}^{t}$ for the substation to satisfy the building heat demand with the given supply temperature, the return temperature $T_{2,i}^{t}$ that can be used to simulate the return network, and a flag w_i^t indicating the feasibility of the configuration. If $w_i^t = 0$, it is not possible to meet the heat demand with the given supply temperature, which should be increased to meet the requirements.

A critical aspect of the procedure lies in the interdependence between the substation and supply network models: to run the substation model and estimate the required mass flow rate, the substation supply temperature is needed, as expressed by Equation (4); however, the supply temperatures of all substations are outputs of the supply network model, which itself requires the mass flow rates from the substations, as detailed Section 2.1.3. To address this issue, an iterative procedure is implemented, as detailed in Section 2.1.4.

2.1.3. Model of the DH network

This section describes the model used to perform the thermo-fluid dynamic simulation of the sub-LTDH. The thermo-fluid dynamic analysis of the network involves the calculation of mass flow rates, pressures, and temperatures along the entire network and has multiple purposes: to estimate the temperature drop between the supply temperature of the network and the supply temperature reaching the substations, which is essential for simulating the substation; to ensure that the configuration is feasible also from a network perspective by analyzing velocities and pressure losses; and, finally, to estimate the operating conditions of the HP in order to calculate the COP.

The adopted model is based on the findings of [30]. It is a physical model based on the solution of the conservation equations of mass, momentum, and energy through the finite volume method, using the upwind scheme to discretize convective fluxes [31]. The model is one dimensional and uses the graph theory [32] to represent the topology of the network: each pipe is modeled as a branch connecting two nodes. The interconnections between nodes and branches are represented in the incidence matrix **A**, which has rows corresponding to nodes and columns corresponding to branches. For a given branch, the matrix entry is 1 if the node is the inlet, −1 if it is the outlet, and 0 if the node and branch are not connected. As previously proposed by other authors [33–35], the analysis in this study is performed under steady-state assumptions. The resulting systems of equations, which can be sequentially applied to the supply and return network, are reported in matrix form in Equations (5)–(7), where the unknown terms are represented by:

- the mass flow rates in the branches, contained in the array **G**;
- the pressures in the nodes, array **P**;
- the temperatures in the nodes, array **T**.

Known terms associated with the characteristics of the network are included in the fluid dynamic conductance matrix **Y**, the stiffness matrix of the thermal problem **K**, the vector accounting for pressure rises $\boldsymbol{\tau}$, the vector taking into account the heat release to the ground **l**. As boundary conditions, for the fluid dynamic problem the pressure in one node is specified, as well as the mass flow rates extraction from the substations which are included in the array $\mathbf{G_{ext}}$ (in the i-th entry, this vector contains the mass flow rate $\dot{m}^t_{p,i}$ required by the corresponding substation); for the thermal problem, the temperature at the inlet nodes must be specified.

$$\mathbf{A}\cdot\mathbf{G}+\mathbf{G_{ext}}=\mathbf{0} \tag{5}$$

$$\mathbf{G}=\mathbf{Y}(\mathbf{G})\cdot\mathbf{A}^{\mathrm{T}}\cdot\mathbf{P}+\mathbf{Y}(\mathbf{G})\cdot\boldsymbol{\tau} \tag{6}$$

$$\mathbf{K}(\mathbf{G})\cdot\mathbf{T}=\mathbf{l} \tag{7}$$

The pressure-velocity coupling in the continuity and momentum equations, expressed in matrix form respectively in Equation (5) and Equation (6), requires a coupled solution of the fluid-dynamic problem in the general case of looped configurations. In these cases, the SIMPLE algorithm is used, as described in Ref. [36]; instead, for simpler networks with tree-shaped topologies, the two systems of equations can be solved sequentially. Once the distribution of mass flow rates in the network is obtained, the thermal problem, expressed by Equation (7), can be obtained by solving a linear system.

The described model is applied separately to the supply and return lines of the network. For the purpose of this analysis, the model can be summarized in two nonlinear functions that contain the information about the network: h_s for the supply line, and h_r for the return line. The required input and the specific outputs which are of interest in this analysis are reported in Equations (8) and (9).

$$T^t_{1,i}=h_s\left(\dot{m}^t_{p,i},T^t_s\right) \tag{8}$$

$$T^t_r=h_r\left(\dot{m}^t_{p,i},T^t_{2,i}\right) \tag{9}$$

From Eq. (8), the model of the supply network, described by the function h_s, allows to obtain the supply temperature of all the substations $T^t_{1,i}$ given the supply temperature of the network T^t_s and the mass-flow rate required by all the buildings $\dot{m}^t_{p,i}$ at a given time t. The mass-flow rate required by all the buildings can be obtained through the substation model, expressed by Eq. (4). However, as discussed in Section 2.1.2, the substation model requires as input the supply temperature of the substations $T^t_{1,i}$, which would be an output of the supply network model itself. For this reason, at iterative procedure is needed, as detailed in Section 2.1.3.

Then, after the coupled solution of the supply network and substation models, the model of the return network described by the function h_r and expressed by Eq. (9) allows to estimate the return temperature of the network T^t_r at time t given the return temperature of all the substations $T^t_{2,i}$ and the mass flow rate required by each of them $\dot{m}^t_{p,i}$.

2.1.4. Flow-chart of the model

In this section, the flow-chart of the model needed to simulate the sub-LTDH network is summarized. As shown in Fig. 5, the procedure involves the following steps:

a) For each time step, the thermal demand of each building connected to the network is estimated according to the regression model described in Section 2.1.1.
b) The supply temperature of the network is guessed, starting from a low value.
c) A simulation of the supply network is carried out through the model described in Section 2.1.3, with guessed values of mass flow rate required by the buildings.
d) From the simulation of the supply network, the supply temperature values at the different substations are calculated. These values are given as input to the substation model (Section 2.1.2), along with the thermal demand calculated at step (a). The model is repeated for each substation and allows estimating the required mass flow rate and the return temperature.
e) The new values of mass flow rate are used to simulate again the supply network, starting again from step (c), until a convergence is reached.
f) If the supply temperature guessed at step (b) is not sufficient to satisfy the thermal demands of all the buildings (according to the feasibility flag w^t_i obtained as output of the substation model), the supply temperature is increased and the procedure is repeated starting from step (b).
g) Otherwise, the solution of the supply network and of the substation model can be considered as definitive and the return network can be simulated to complete the solution of the entire system.

At the end of the procedure, a complete solution of the system is obtained. For each time step of the analyzed period, the minimum value of supply temperature required by the system can be predicted, along with accurate estimations of mass flow rates, pressures, and temperatures in all branches/nodes of the system. These estimations make it possible to assess the feasibility of the system from a network perspective (e.g., by evaluating velocities and pressures within the system) and to estimate the performance of the distributed production unit to be installed, which in this case is a GWHP (Section 2.2).

2.2. Operation of the heat pump

To simulate the operation of the HP, the simplified model proposed by Reinholdt et al. [37] is adopted. The Coefficient of Performance (COP) is estimated through the Lorenz-Efficiency η_{Lor}, which is supposed to be constant, according to Equation (10), where $T^t_{lm,H}$ and $T^t_{lm,L}$ represent the logarithmic mean temperature of respectively the sink (DH network) and the source (groundwater) at time t.

$$COP^t_{HP}=\eta_{Lor}COP^t_{Lor}=\eta_{Lor}\frac{T^t_{lm,H}}{T^t_{lm,H}-T^t_{lm,L}} \tag{10}$$

In this study, it is supposed that the GWHP is installed in an area in which the groundwater is not affected by the presence of other groundwater installations. For this reason, the groundwater temperature is assumed constant and equal to the undisturbed value. Nevertheless, the model can be effectively coupled with a groundwater flow model to

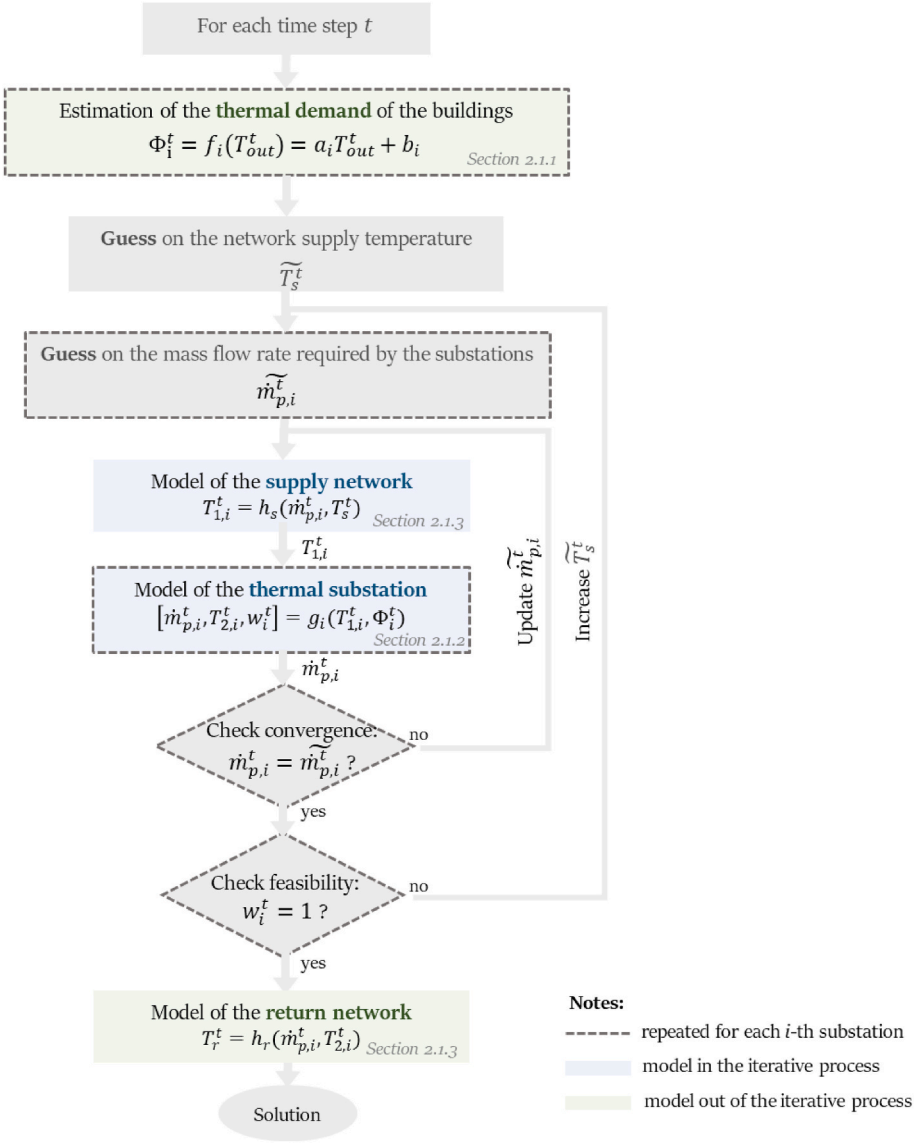

Fig. 5. Flow chart of the model for the simulation of the sub-LTDH network.

assess how the COP changes according to the groundwater temperature and, consequently, to estimate the influence of the chosen installation site in case of interference between neighboring systems [38,39]. This potential interference should not be seen only in a negative way, while it can turn into positive effects in case of careful selection of the site, which can also allow using the groundwater as a seasonal storage medium [40].

The power input required by the HP is estimated as expressed in Equation (11), where T_{HP}^t represents the supply temperature of the HP at time t, T_r^t the return temperature from the sub-LTDH, and $\dot{m}_{HP}^t$ the mass flow rate processed by the HP.

$$W_{HP}^t = \frac{\Phi_{HP}^t}{COP_{HP}^t} = \frac{\dot{m}_{HP}^t \, c_p \left(T_{HP}^t - T_r^t\right)}{COP_{HP}^t} \tag{11}$$

The supply temperature of the HP is constrained by an upper limit, supposed in this study equal to 80 °C. When the supply temperature of the sub-LTDH is higher than this threshold, a boost is required from the master network. Thus, part of the mass flow rate required by the sub-LTDH is taken from the master network (at higher temperature T_{MN}^t) and mixed to the flow rate processed by the HP. The mass flow rate required by the master network $\dot{m}_{MN}^t$ and the mass flow rate processed by the HP $\dot{m}_{HP}^t$ can be easily calculated from a mass and energy balance, as described by Equations (12) and (13), where $\dot{m}_{tot}^t$ is the total mass flow rate required by the sub-LTDH at time t, which is an output of the model described in Section 2.1.

$$\dot{m}_{HP}^t + \dot{m}_{MN}^t = \dot{m}_{tot}^t \tag{12}$$

$$\dot{m}_{HP}^t T_{HP}^t + \dot{m}_{MN}^t T_{TN}^t = \dot{m}_{tot}^t T_s \tag{13}$$

3. Case study

This study focuses on a large-scale DH network located in Northern Italy, serving over 6500 buildings across multiple neighborhoods in various city zones. The customers are predominantly residential users in apartment buildings connected to DH for space-heating purposes only. Currently, the network is powered by combined heat and power (CHP) plants, which deliver pressurized hot water at a supply temperature of 120 °C; thermal storage units and heat-only boilers are used to cover the peak loads. The return temperature fluctuates around 60 °C, adjusting dynamically to the heating loads of the connected buildings. During cold winter days, the system experiences a demand of approximately 1 GW in steady-state conditions, with morning peaks reaching up to 1.4 GW.

These peaks are associated with the common operational practice among users in Mediterranean regions of switching off heating devices during nighttime hours to reduce energy consumption.

In this paper, three potential sub-systems are identified for potential installation of GWHPs and transition to lower supply temperatures with a dynamic supply temperature approach, keeping the temperature of the master network at 120 °C. The topology of the three sub-LTDH networks is represented in Fig. 6:

- Network (a) serves 66 buildings;
- Network (b) serves 50 buildings;
- Finally, network (c) serves 87 buildings.

The selected subsystems were selected among those with sufficient data availability and in consideration of the characteristics of the area, to ensure that operational changes would not compromise customer thermal comfort. Nevertheless, the analysis method can be extended to all subsystems with adequate data availability. Furthermore, the proposed methodology is designed to be flexible and transferable to other district heating contexts, provided that sufficient input data is available. This makes it applicable to a wide range of networks with different sizes and layouts.

The HP is supposed to be installed at the connection point with the master network, highlighted in red in the figure. The systems are active only during the heating season, which lasts from October 15th to April 15th in the city in question. The analysis is performed for 8 heating seasons, whose outdoor temperature is shown in Fig. 7 with a time step of 5 min. The heating systems are generally operating from around 6 a.m. to 10 p.m.; in this analysis, the start-up time is anticipated to a cautionary value (different for each day, according to the outdoor temperature) that allows respecting the total energy required by the buildings even if considering steady-state conditions only.

In the selected areas, a shallow aquifer is present, and the undisturbed groundwater temperature is about 15 °C.

4. Results and discussion

This section is dedicated to the presentation and discussion of the results of the analysis.

4.1. Current scenario: high-temperature supply

For comparison purposes, the current high-temperature scenario in the three networks is first simulated. The operation of the network is represented in Fig. 8. The supply temperature is the same for the three networks, equal to 120 °C and constant regardless of the outdoor conditions. The systems are regulated by controlling the mass flow rate, which automatically adapts to the demand of the buildings, decreasing as the outdoor temperature increases and the heat demand decreases. The return temperature varies in the range 30–80 °C according to the operation of the substations and decreases as the mass flow rate decreases.

Fig. 9 illustrates the operation of the substations, showing two sample substations for each network. The trends in supply temperature, return temperature, and mass flow rate follow a similar pattern to those observed at the network level. The supply temperature of the network can be compared to the supply temperature of the substation, where a temperature drop occurs due to distribution losses. While the supply temperature of the network remains constant, the supply temperature of the substation decreases as the outdoor temperature increases. This is due to the increasing heat losses as the mass flow rate decreases. This temperature drop is moderate for substations (a1), (b1), and (c1), which are closer to the connection point, while it is more pronounced for substations (a2), (b2), and (c2), which are further away. In these cases the temperature drops by almost 20 °C in the most critical condition. Reducing supply temperatures and increasing the mass flow rate can not only help to integrate renewables, but also to reduce this significant temperature drop in the mid-season.

4.2. Improved scenario: variable low-temperature supply

In this section, the results of the model discussed in Section 2.1 are presented and the operation of the three sub-LTDH networks with the proposed dynamic temperature approach is analyzed.

The modified operation of the three sub-LTDH networks is illustrated in Fig. 10. Two different parts can be distinguished in each graph:

- On the left side of the graph, when the outdoor temperature is lower than a certain value – which is around −1 °C in Network (a) and Network (b), and around −4 °C in Network (c) – the system continues to operate as in the high-temperature scenario. Due to the request of one or more buildings, the supply temperature cannot be lower than 120 °C. In these conditions, the master network continues to fully supply the subsystem, with a constant supply temperature and an increasing mass flow rate as the outdoor temperature decreases.
- On the right part of the graph, the supply temperature is reduced, and the dynamic temperature approach can be implemented. As the outdoor temperature increases, the supply temperature can be

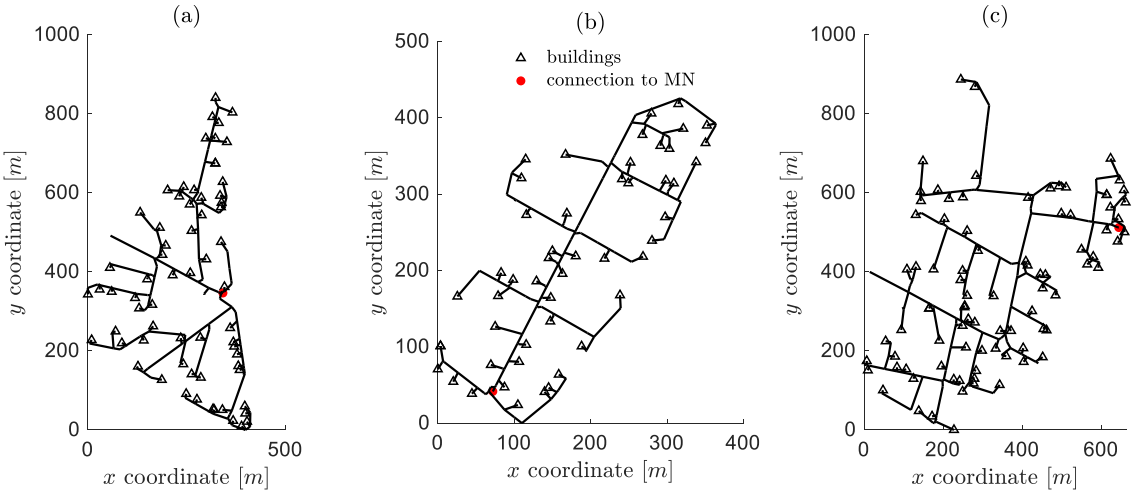

Fig. 6. Topology of the three sub-networks analyzed; the connection point to the master network (MN) is highlighted with a red bullet. (For interpretation of the references to colour in this figure legend, the reader is referred to the Web version of this article.)

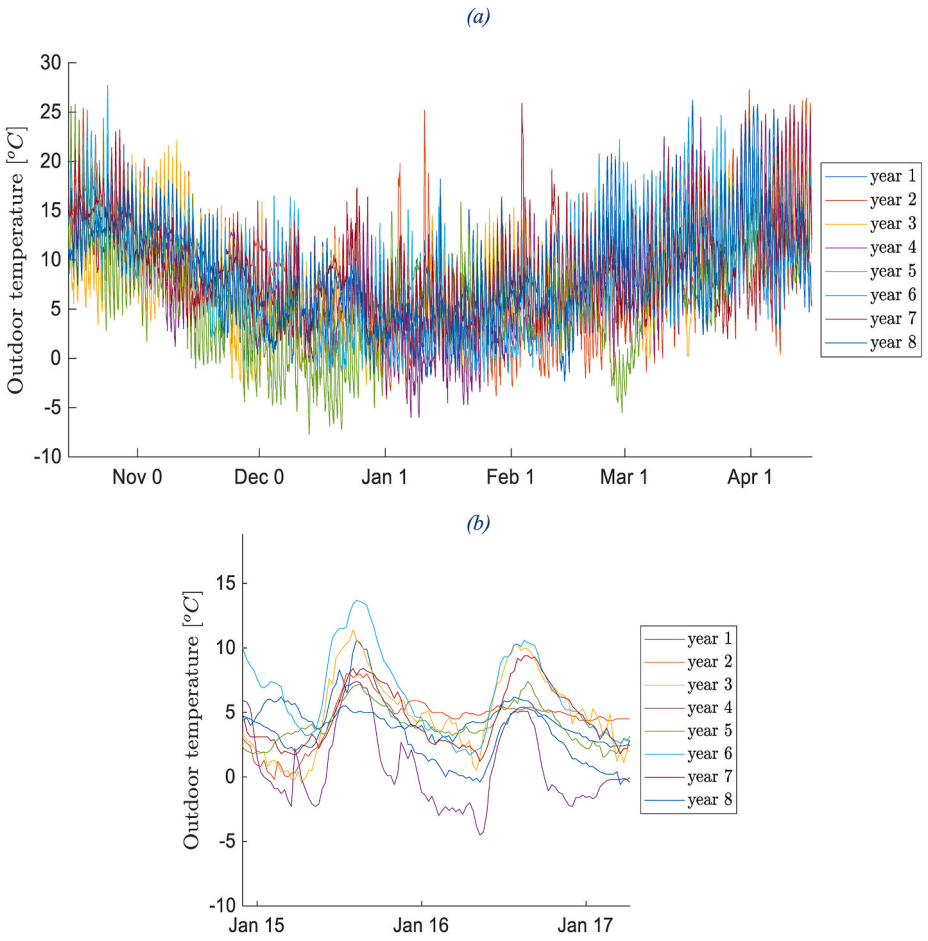

Fig. 7. Evolution of the outdoor temperature for the 8 years analyzed (a) during the whole heating season (b) during two representative days.

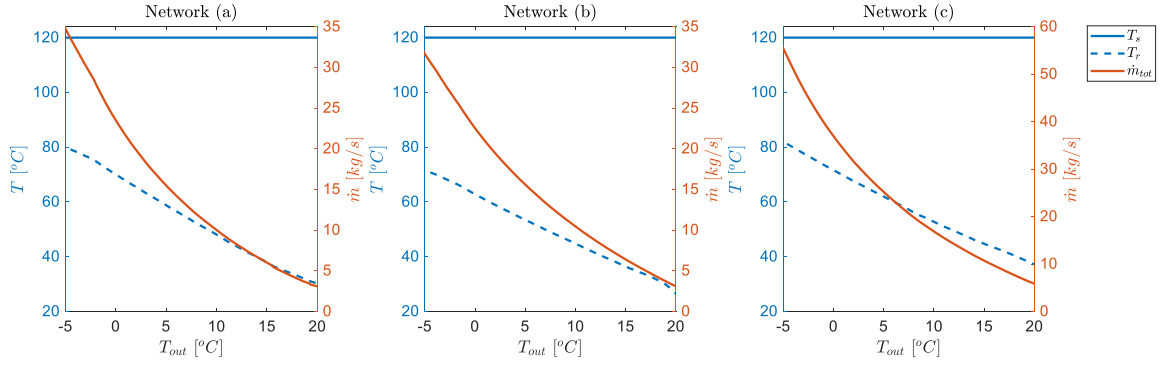

Fig. 8. Current high-temperature scenario: supply temperature, return temperature, and total mass flow rate of each network under varying outdoor conditions.

lowered according to the requirements of the buildings. This value of supply temperature at network level is determined by a critical user, which is not necessarily the user with the highest temperature demand at given outdoor temperature, but rather the one that imposes the highest temperature requirement on the network, taking into account also the temperature losses along the distribution network. In this critical substation, the mass flow rate reaches its maximum value, and a higher supply temperature is required to meet the thermal demand under specific outdoor conditions. The critical user can change depending on outdoor conditions and on the operation of the whole system: a change in the slope of the curve may indicate a transition to a different critical user within the system. The return temperature has a decreasing trend as the outdoor temperature increases. Finally, the mass-flow rate shows a non-monotonous behavior, which will be better explained in the discussion of Figs. 11 and 12.

The operation of the three sample substations with the new operating conditions is represented in Fig. 11: in contrast to the high-temperature scenario (Fig. 9), the temperature losses are significantly reduced in this case, especially at high outdoor temperatures, which are the most problematic in the current operating conditions. This is due to both the lower temperatures and the higher mass flow rates involved. As a result, the temperature difference between the system supply and the substation supply never exceeds 6 °C in Network (a), 2 °C in Network (b), and 7 °C in Network (c).

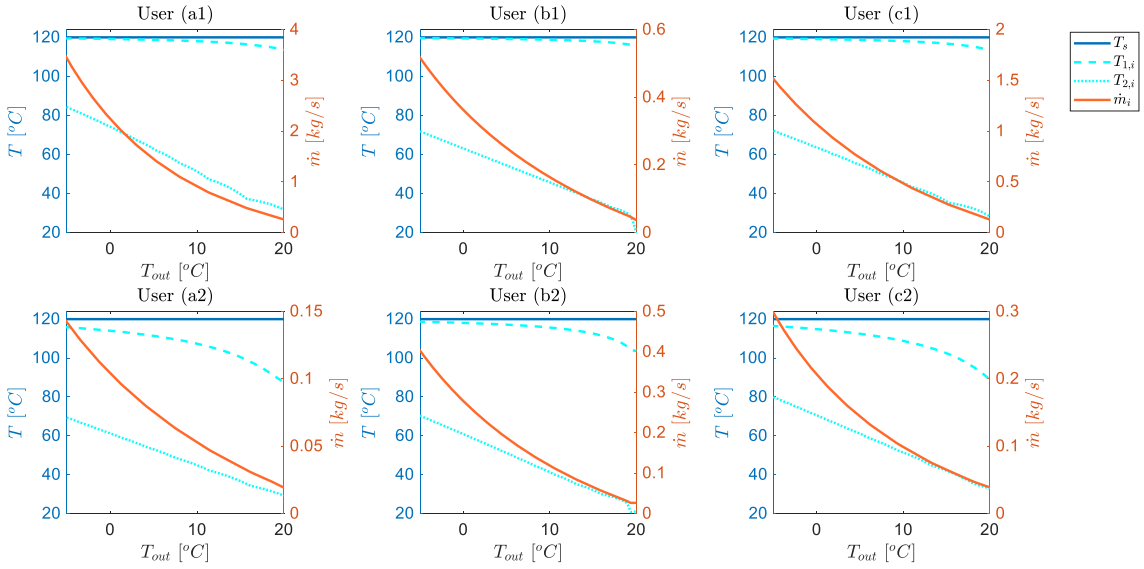

Fig. 9. Current high-temperature scenario: supply temperature of the network; supply temperature, return temperature, and mass flow rate of two sample substations for each network under varying outdoor conditions.

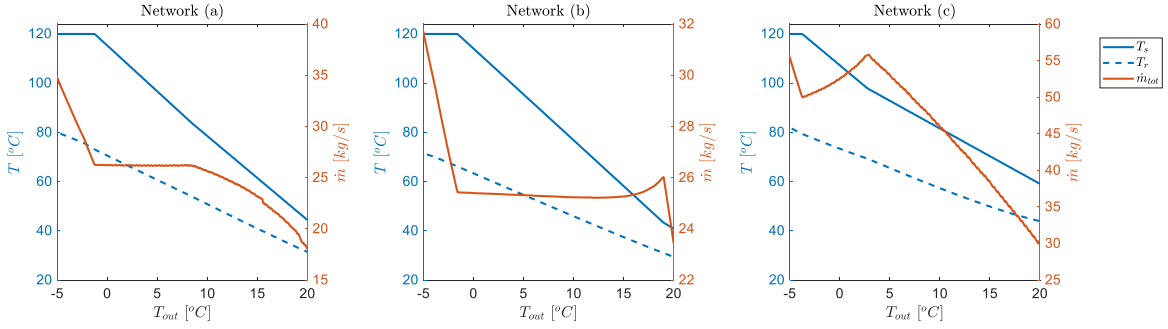

Fig. 10. Improved low-temperature scenario with dynamic temperature supply: supply temperature, return temperature, and total mass flow rate of each network under varying outdoor conditions.

In terms of mass flow rates, it is not straightforward to determine how substation mass flows evolve using this dynamic temperature approach. In fact, this is a result of all the complex dynamics that occur at both the substation and network levels. Although the trend is generally decreasing as the outdoor temperature increases and the heat demand decreases, a different behavior can be observed in specific situations. An example is illustrated in Fig. 12, where the minimum supply temperature required by a given substation in the different outdoor conditions is reported in green. For those conditions where the specific substation does not represent the critical user, this value is lower than the actual supply temperature of the substation, which is instead determined by other critical buildings and by the dynamics of the overall system. The increasing or decreasing trend of the mass flow rate with increasing outdoor temperature depends on the relative slopes of these two temperature curves and on the characteristics of the substation: in the case of User (b3), shown in Fig. 12, the difference between the actual supply temperature and the minimum required supply temperature undergoes a significant increase as the outdoor temperature decreases; since the supply temperature is increasingly much higher than the required value, the mass flow rate decreases as the outdoor temperature decreases. The resulting trend at network level (visible in Fig. 10) depends on the prevalence and impact of these cases.

In general, the mass flow rates are higher compared to the high-temperature scenario. This results in higher velocities and pumping costs. The thermo-fluid dynamic simulation of the network makes it possible to guarantee that threshold values are not exceeded. As an example of the results from the fluid-dynamic model, Fig. 13 presents the velocity distribution at $T_{out} = 0\ °C$ for the three sub-LTDH networks. In these conditions, the velocity is below 0.9 m/s in all the pipes.

The assessment of heat losses is another key output of the thermo-fluid dynamic model. In Fig. 14, they are reported as a percentage of the total heat load as a function of the outdoor temperature. As the outdoor temperature increases, the total heat load decreases making heat losses in the distribution network more significant in relative terms. In the current high-temperature scenario, they range between 2 % and 13 % depending on the network and outdoor conditions. In contrast, the proposed configuration reduces these losses to just 2–6 % of the total heat load. The reduction is more pronounced for high outdoor temperatures, where the supply temperature is reduced the most, while no reduction is observed in those conditions where the network continues to operate at the same temperature level. In absolute terms, the proposed approach results in thermal energy savings of approximately 110 MWh, 80 MWh, and 200 MWh per heating season for networks (a), (b), and (c), respectively.

From the results of the sub-LTDH model, the supply temperature of each network during each heating season can be obtained. As an example, the solution for the first heating season is presented in Fig. 15. Unlike the current scenario with fixed supply temperature, the proposed

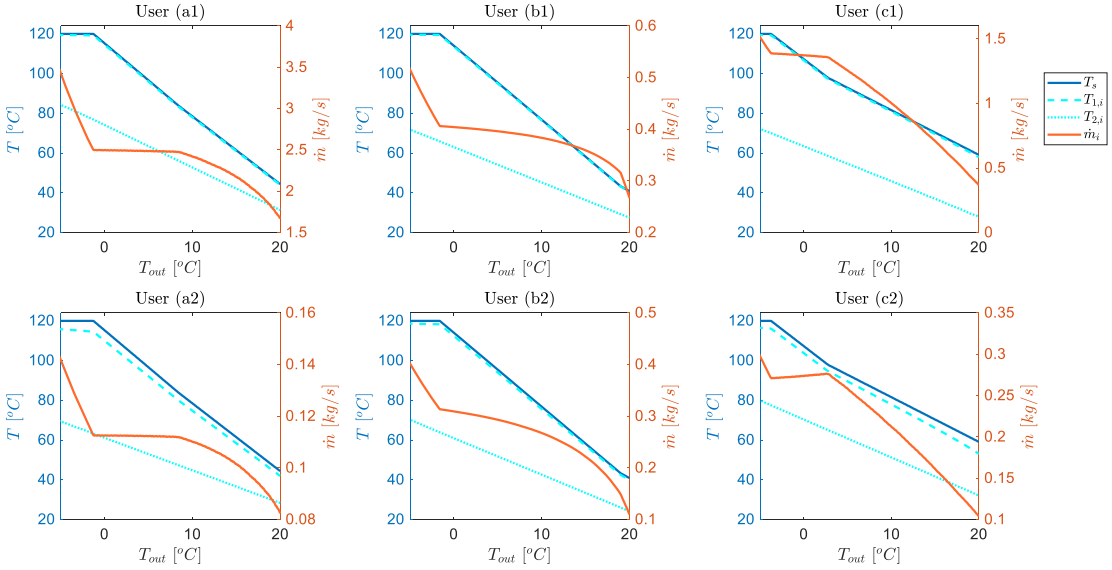

Fig. 11. Improved low-temperature scenario with dynamic temperature supply: supply temperature of the network; supply temperature, return temperature, and mass flow rate of two sample substations for each network under varying outdoor conditions.

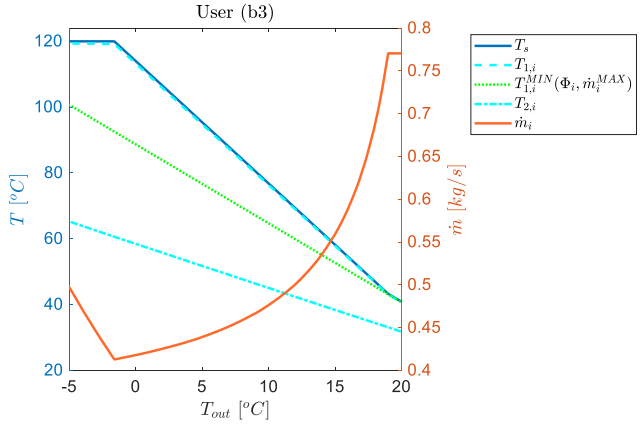

Fig. 12. Improved low-temperature scenario with dynamic temperature supply: supply temperature of the network; supply temperature, minimum supply temperature, return temperature, and mass flow rate of two sample substations for each network under varying outdoor conditions.

approach dynamically adjusts to the demand of each system. It is possible to see that during the heating season considered, the current supply temperature of 120 °C is never required. This result becomes even more significant when it is considered that the conditions on the secondary side of the substations are not changed. This means that even greater changes could be made if it were considered to improve the operation of the substations and/or of the buildings as well. Among the three networks, Network (c) exhibits the highest value of the minimum supply temperature during the year, but it is also the one with the lowest maximum values.

From the temperature evolution over time, it is possible to obtain the temperature duration curve, which represents the temperature values in relation to how long they remain above a specific value. This curve is shown in Fig. 16 for all 8 heating seasons analyzed. From this figure, it can be seen that all the networks can operate at temperatures below 90 °C for more than half of the operating time in all the years analyzed, including year 5 that is the coldest and the most critical.

4.3. Operation of the GWHP

In this section, the results of the model of the GWHP are presented. It is assumed that the GWHP can provide supply water up to 80 °C, while for higher supply temperature an integration for the master network is needed.

In Fig. 17, the total mass flow rate required by each sub-LTDH network is divided into two components: the mass flow rate supplied by the GWHP and the mass flow rate required from the master network. This distinction highlights the contribution of each source in meeting the demand of the systems. When the outdoor temperature is higher than approximately 10 °C, the GWHP is able to fully satisfy the demand of the three networks. As the outdoor temperature decreases, the mass flow rate provided by the GWHP gradually decreases and an increasing contribution from the master network, operating at 120 °C, is needed to reach the temperature level required by the systems.

This solution offers advantages from multiple perspectives: in addition to the integration of renewable energy sources in the local sub-LTDH networks, the master network itself benefits from a reduction in the mass flow rate compared to the high-temperature scenario. This reduces the hydraulic bottlenecks, boosting the capabilities of network expansion to new areas of the city and enhancing the reduction of operating temperatures in the master network itself.

The COP of the GWHP is shown in Fig. 18(a) as a function of the outdoor temperature: it varies from around 3 when the outdoor temperature is very low (−5 °C) up to 7.8, 8.1, and 4.8 respectively for networks (a), (b), and (c) at higher outdoor temperatures (20 °C). The lower performance of network (c) is due to the higher values of the minimum supply temperatures. The corresponding Seasonal Coefficient of Performance (SCOP), calculated for the 8 years included in the analysis, is reported in Fig. 18(b), where a slight decrease in year 5 can be observed due to colder outdoor temperatures.

The performance of the GWHP may be further boosted by choosing a proper location for the extraction well: the exploitation of positive thermal perturbations in the groundwater temperature allows to obtain an increase in the COP.

In terms of heat demand, Fig. 19 shows the proportion provided by the GWHP and the master network as a function of the outdoor temperature: the GWHP provides its maximum heat demand when the outdoor temperature is sufficiently high to avoid any boost from the

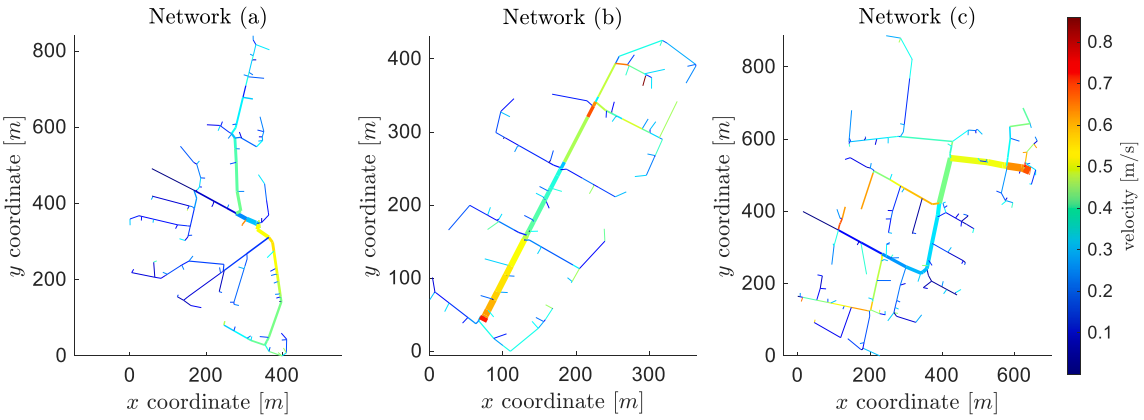

Fig. 13. Improved low-temperature scenario: velocity distribution in the three networks at $T_{out} = 0\ °C$; the width of each branch is proportional to the mass flow rate flowing in the corresponding pipe.

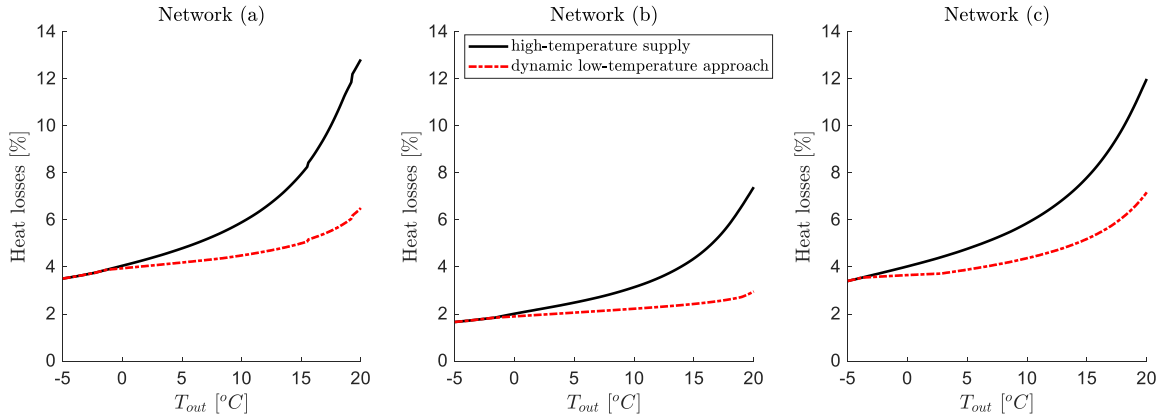

Fig. 14. Comparison of heat losses in the high-temperature and low-temperature scenarios.

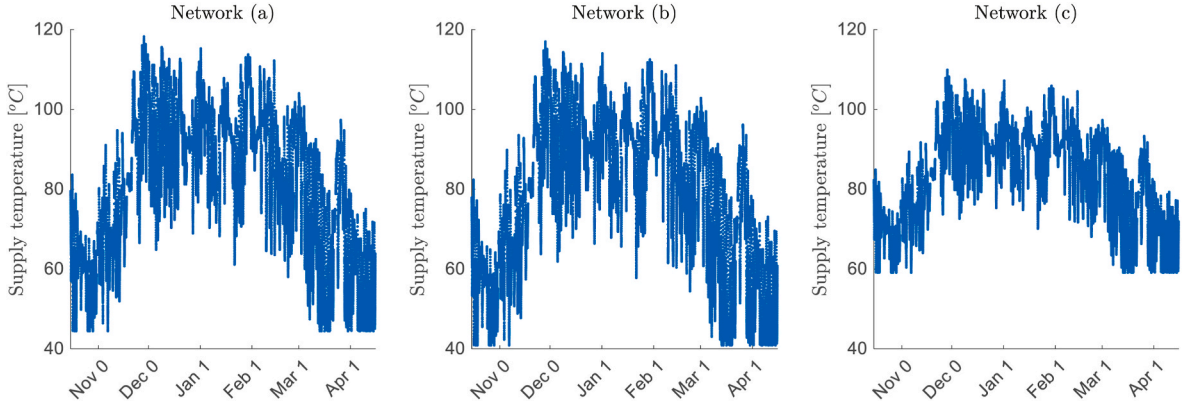

Fig. 15. Supply temperature of the three networks with the dynamic temperature approach – year 1.

high-temperature master network. The combination of these profiles with the evolution of the outdoor temperature in the 8 analyzed heating seasons allows to obtain the share of thermal energy provided by both, illustrated in Fig. 20. With the exception of year 5, where the share provided by the GWHP is in the range 43–46 % depending on the network, it is always above 50 % in the other heating seasons and reaches almost 70 % in year 7. Assuming that the HP is powered by renewable electricity, this share can be considered as entirely renewable. This is a significant result, which becomes even more important when one considers that renewable thermal energy was assumed to be available only at temperatures below 80 °C; with renewable production at higher temperatures, the percentage can increase further.

5. Conclusions

The transition towards low-carbon and renewable-based District Heating (DH) networks is crucial to achieving climate neutrality targets by 2050. However, integrating low-temperature renewable heat sources

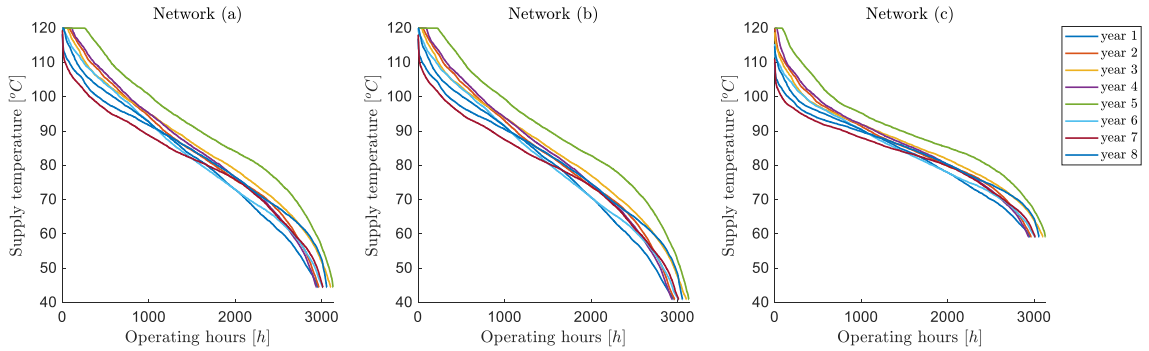

Fig. 16. Temperature duration curve of the three networks with the dynamic temperature approach.

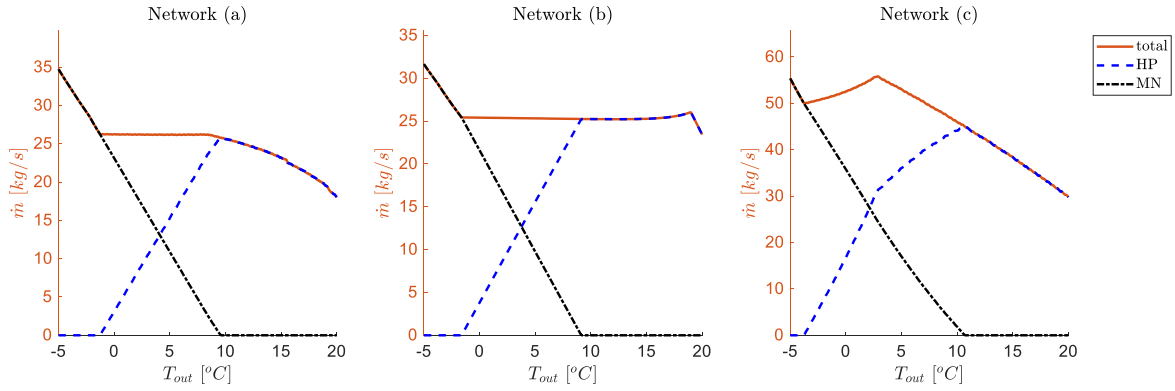

Fig. 17. Total mass flow rate required by each sub-LTDH network, mass flow rate provided by the GWHP, and mass flow rate required by the master network as a function of the outdoor temperature.

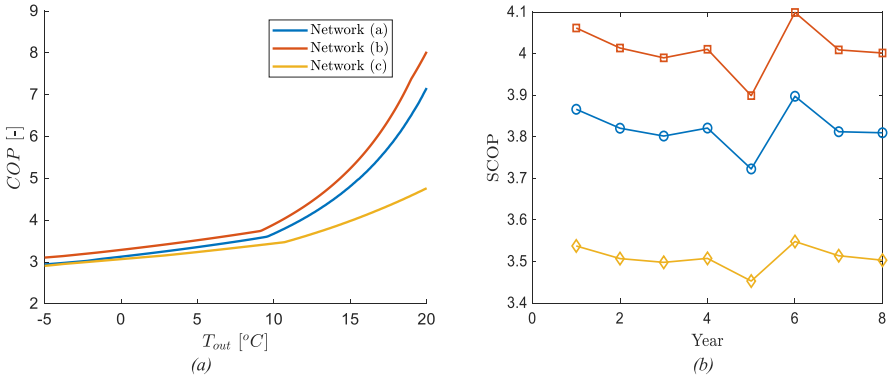

Fig. 18. COP of the GWHP for different outdoor temperatures (a) and SCOP in the 8 heating seasons (b).

into large-scale DH networks originally designed for high-temperature fossil-fuel operations presents significant technical and economic challenges. This study proposes a viable pathway for this transition through the implementation of low-temperature sub-networks (sub-LTDH) powered by decentralized renewable energy sources, specifically groundwater heat pumps (GWHPs).

By developing a comprehensive methodology that integrates a) a thermo-fluid dynamic model of the DH network, b) simulations of the operation of the substations, and c) performance analysis of the GWHPs, this study proposes a useful tool for the decarbonization of existing networks. Moreover, through an application to a real large-scale system, the work shows that the three sub-LTDH networks can effectively operate at reduced supply temperatures for over half of the operating conditions analyzed. This result indicates that the proposed system can function predominantly on renewable heat, requiring support from the master DH network, which is currently supplied by combined heat and power plants and operating at high temperatures, only for limited time.

Key findings of this research include:

- The feasibility of lowering DH network operating temperatures while maintaining the required heat supply to connected buildings.
- The importance of accurately modeling the thermo-fluid dynamic response of the networks to ensure sustainable operation.
- The ability of GWHPs to enhance renewable heat integration, improving overall system efficiency and reducing dependence on fossil fuels.

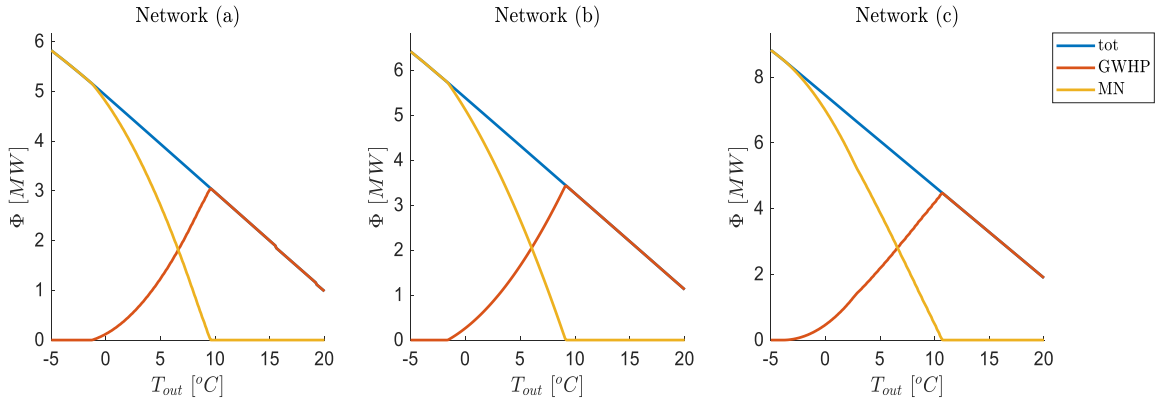

Fig. 19. Total heat load of the three sub-LTDH networks, heat load supplied by the GWHP, and heat load provided by the master network as a function of the outdoor temperature.

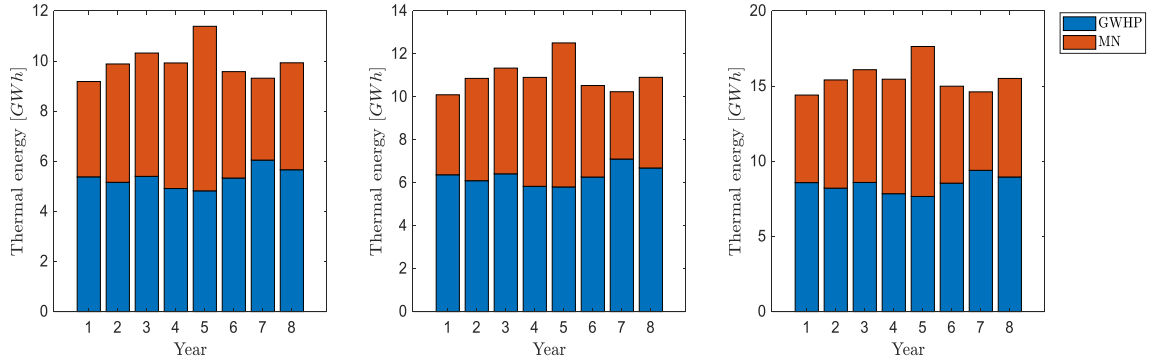

Fig. 20. Thermal energy provided by both GWHP and master network in the 8 heating seasons analyzed.

- The role of dynamic supply temperature management in optimizing DH network performance, minimizing energy losses, and maximizing renewable energy utilization.

Although the work confirms the technical feasibility of the proposed approach in the specific application, it also provides a comprehensive methodology that can support DH operators and policymakers in planning the gradual transition of existing networks. The methodology is suitable for application to other DH systems with varying configurations, climate conditions, and renewable resource availability. Future analyses could include different renewable production technologies, adapting to the characteristics of each system and location.

Overall, this work provides a strong foundation for the gradual decarbonization of existing DH networks by exploiting sub-LTDH as a transition strategy, thereby contributing to the broader goal of achieving a sustainable and resilient energy future.

CRediT authorship contribution statement

Martina Capone: Writing – review & editing, Writing – original draft, Visualization, Software, Methodology, Data curation, Conceptualization. **Marco Canino:** Software, Methodology. **Elisa Guelpa:** Writing – review & editing, Methodology, Funding acquisition, Conceptualization.

Declaration of competing interest

The authors declare that they have no known competing financial interests or personal relationships that could have appeared to influence the work reported in this paper.

Acknowledgement

This study was carried out within the «REVEDH: REVolutionary changE of Vision for District Heating: holistic approach to realistically reach 100 % renewable networks » project – funded by the Ministero dell'Università e della Ricerca – within the PRIN 2022 program (D. D.104–02/02/2022) and European Union – Next Generation EU. This manuscript reflects only the authors' views and opinions and the Ministry cannot be considered Responsible for them.

References

[1] A. Adamo, H. Martín, J. de la Hoz, J. Rubio, J. Valero, Regulatory framework for the promotion of heat pumps in the European union, Energy Rep. 12 (Dec. 2024) 5909–5930, https://doi.org/10.1016/J.EGYR.2024.11.043.
[2] E. Mäki, L. Kannari, I. Hannula, J. Shemeikka, Decarbonization of a district heating system with a combination of solar heat and bioenergy: a techno-economic case study in the northern European context, Renew. Energy 175 (Sep. 2021) 1174–1199, https://doi.org/10.1016/J.RENENE.2021.04.116.
[3] International Energy Agency, Renewable Heat, 2021, https://doi.org/10.1016/s1471-0846(05)00330-6.
[4] A. Hast, S. Syri, V. Lekavičius, A. Galinis, District heating in cities as a part of low-carbon energy system, Energy 152 (Jun. 2018) 627–639, https://doi.org/10.1016/J.ENERGY.2018.03.156.
[5] S. Frederiksen, S. Werner, District Heating and Cooling, Studentlitteratur AB, 2013.
[6] S. Werner, International review of district heating and cooling, Energy 137 (2017) 617–631, https://doi.org/10.1016/j.energy.2017.04.045.
[7] M. Sameti, F. Haghighat, Optimization of 4th generation distributed district heating system: design and planning of combined heat and power, Renew. Energy 130 (Jan. 2019) 371–387, https://doi.org/10.1016/J.RENENE.2018.06.068.
[8] H. Lund, et al., The status of 4th generation district heating: research and results, Energy 164 (2018) 147–159, https://doi.org/10.1016/j.energy.2018.08.206.
[9] Y. Xu, C. Zhan, A.R. Jensen, M. Gao, W. Kong, J. Fan, Thermo-economic analysis of a solar district heating plant with an air-to-water heat pump, Renew. Energy 237 (Dec. 2024) 121490, https://doi.org/10.1016/J.RENENE.2024.121490.

[10] M. Capone, E. Guelpa, V. Verda, Optimal installation of heat pumps in large district heating networks, Energies 16 (2023) 1448.
[11] P. Sdringola, et al., Prosumers and district heating: experimental validation of strategies to improve thermal energy production and consumption, Energy Build. 338 (Jul. 2025) 115713, https://doi.org/10.1016/J.ENBUILD.2025.115713.
[12] H. Averfalk, P. Ingvarsson, U. Persson, M. Gong, S. Werner, Large heat pumps in Swedish district heating systems, Renew. Sustain. Energy Rev. 79 (May) (2017) 1275–1284, https://doi.org/10.1016/j.rser.2017.05.135.
[13] J.S. Figueira, et al., Shallow geothermal energy systems for district heating and cooling networks: review and technological progression through case studies, Renew. Energy 236 (Dec. 2024) 121436, https://doi.org/10.1016/J.RENENE.2024.121436.
[14] P.A. Østergaard, A.N. Andersen, Booster heat pumps and central heat pumps in district heating, Appl. Energy 184 (2016) 1374–1388, https://doi.org/10.1016/j.apenergy.2016.02.144.
[15] H. Lund, et al., 4th Generation District Heating (4GDH). Integrating smart thermal grids into future sustainable energy systems, Energy 68 (2014) 1–11, https://doi.org/10.1016/j.energy.2014.02.089.
[16] M. Gong, S. Werner, Exergy analysis of network temperature levels in Swedish and Danish district heating systems, Renew. Energy 84 (Dec. 2015) 106–113, https://doi.org/10.1016/J.RENENE.2015.06.001.
[17] E. Guelpa, M. Capone, A. Sciacovelli, N. Vasset, R. Baviere, V. Verda, Reduction of supply temperature in existing district heating: a review of strategies and implementations, Energy 262 (Jan. 2023) 125363, https://doi.org/10.1016/J.ENERGY.2022.125363.
[18] Y. Merlet, R. Baviere, N. Vasset, Optimal retrofit of district heating network to lower temperature levels, Energy 282 (Nov. 2023) 128386, https://doi.org/10.1016/J.ENERGY.2023.128386.
[19] L. Socci, A. Rocchetti, A. Verzino, A. Zini, L. Talluri, Enhancing third-generation district heating networks with data centre waste heat recovery: analysis of a case study in Italy, Energy 313 (Dec. 2024) 134013, https://doi.org/10.1016/J.ENERGY.2024.134013.
[20] J. Stock, T. Schmidt, A. Xhonneux, D. Müller, Optimisation of district heating transformation for the efficient integration of a low-temperature heat source, Energy 308 (Nov. 2024) 132461, https://doi.org/10.1016/J.ENERGY.2024.132461.
[21] A. Volkova, et al., Cascade sub-low temperature district heating networks in existing district heating systems, Smart Energy 5 (Feb. 2022) 100064, https://doi.org/10.1016/J.SEGY.2022.100064.
[22] S. Puschnigg, G. Jauschnik, S. Moser, A. Volkova, M. Linhart, A review of low-temperature sub-networks in existing district heating networks: examples, conditions, replicability, Energy Rep. 7 (Oct. 2021) 18–26, https://doi.org/10.1016/J.EGYR.2021.09.044.
[23] A. Volkova, et al., Energy cascade connection of a low-temperature district heating network to the return line of a high-temperature district heating network, Energy 198 (2020), https://doi.org/10.1016/j.energy.2020.117304.
[24] P. Friedrich, T. Huynh, S. Niessen, Optimizing district heating operations: network modeling and its implications on system efficiency and operation, Smart Energy 18 (May 2025) 100175, https://doi.org/10.1016/J.SEGY.2025.100175.
[25] A. Zajacs, et al., Utilization of geothermal energy: new possibilities for district heating networks in the Baltic States, Renew. Energy (Jan. 2025) 122375, https://doi.org/10.1016/J.RENENE.2025.122375.
[26] D. xi Liu, H.Y. Lei, J.S. Li, C. shan Dai, R. Xue, X. Liu, Optimization of a district heating system coupled with a deep open-loop geothermal well and heat pumps, Renew. Energy 223 (Mar. 2024) 119991, https://doi.org/10.1016/J.RENENE.2024.119991.
[27] C.S. Blázquez, V. Verda, I.M. Nieto, A.F. Martín, D. González-Aguilera, Analysis and optimization of the design parameters of a district groundwater heat pump system in Turin, Italy, Renew. Energy 149 (Apr. 2020) 374–383, https://doi.org/10.1016/J.RENENE.2019.12.074.
[28] W. Pophillat, G. Attard, P. Bayer, J. Hecht-Méndez, P. Blum, Analytical solutions for predicting thermal plumes of groundwater heat pump systems, Renew. Energy 147 (Mar. 2020) 2696–2707, https://doi.org/10.1016/J.RENENE.2018.07.148.
[29] M. Capone, E. Guelpa, V. Verda, Potential for supply temperature reduction of existing district heating substations, Energy 285 (Dec. 2023) 128597, https://doi.org/10.1016/J.ENERGY.2023.128597.
[30] M. Capone, E. Guelpa, V. Verda, Accounting for pipeline thermal capacity in district heating simulations, Energy 219 (Mar. 2021) 119663, https://doi.org/10.1016/J.ENERGY.2020.119663.
[31] F.P. Incropera, D.P. Dewitt, Fundamentals of Heat and Mass Transfer, 2011.
[32] F. Harary, Graph Theory, Narosa Publishing, New Delhi, 1995.
[33] H. Bahlawan, et al., Detection and identification of faults in a District Heating Network, Energy Convers. Manag. 266 (Aug. 2022) 115837, https://doi.org/10.1016/J.ENCONMAN.2022.115837.
[34] D. Jakubek, P. Ocłoń, M. Nowak-Ocłoń, M. Sułowicz, P.S. Varbanov, J.J. Klemeš, Mathematical modelling and model validation of the heat losses in district heating networks, Energy 267 (Mar. 2023) 126460, https://doi.org/10.1016/J.ENERGY.2022.126460.
[35] L. Manservigi, H. Bahlawan, E. Losi, M. Morini, P.R. Spina, M. Venturini, A diagnostic approach for fault detection and identification in district heating networks, Energy 251 (Jul. 2022) 123988, https://doi.org/10.1016/J.ENERGY.2022.123988.
[36] E. Guelpa, A. Sciacovelli, V. Verda, Thermo-fluid dynamic model of large district heating networks for the analysis of primary energy savings, Energy 184 (2019) 34–44, https://doi.org/10.1016/j.energy.2017.07.177.
[37] L. Reinholdt, et al., Heat pump COP, part 1: generalized method for screening of system integration potentials, Refrig. Sci. Technol. (2018) 1207–1213, https://doi.org/10.18462/iir.gl.2018.1380, 2018-June.
[38] S. Halilovic, F. Böttcher, K. Zosseder, T. Hamacher, Optimizing the spatial arrangement of groundwater heat pumps and their well locations, Renew. Energy 217 (Nov. 2023) 119148, https://doi.org/10.1016/J.RENENE.2023.119148.
[39] D. Park, E. Lee, D. Kaown, S.S. Lee, K.K. Lee, Determination of optimal well locations and pumping/injection rates for groundwater heat pump system, Geothermics 92 (May 2021) 102050, https://doi.org/10.1016/J.GEOTHERMICS.2021.102050.
[40] A. Hesaraki, S. Holmberg, F. Haghighat, Seasonal thermal energy storage with heat pumps and low temperatures in building projects—A comparative review, Renew. Sustain. Energy Rev. 43 (Mar. 2015) 1199–1213, https://doi.org/10.1016/J.RSER.2014.12.002.